Journal of Neuroimmunology 398 (2025) 578488

Contents lists available at ScienceDirect

Journal of Neuroimmunology

journal homepage: www.elsevier.com/locate/jneuroim

Short Communication

Immune cell-enriched single-cell RNA sequencing unveils the interplay between infiltrated CD8$^+$ T resident memory cells and choroid plexus epithelial cells in Alzheimer's disease

Seong-Jun Kang [a,b,1], Yong-Hee Kim [c,1], Thuy Nguyen-Phuong [a,b,c,d,f,1], Yijoon Kim [d], Jin-Mi Oh [e], Jae-chun Go [c], DaeSik Kim [b,c], Chung-Gyu Park [a,b,c,d,f,***], Hyunsu Lee [g,i,**], Hyun Je Kim [a,b,c,d,f,h,*]

[a] Department of Biomedical Sciences, Seoul National University Graduate School, Seoul, Republic of Korea
[b] PB Immune Therapeutics Inc., Seoul, Republic of Korea
[c] Transplantation Research Institute, Medical Research Center, Seoul National University, Seoul, Republic of Korea
[d] Department of Microbiology and Immunology, College of Medicine, Seoul National University, Seoul, Republic of Korea
[e] Samsung Genomic Institute, Samsung Medical Center, Seoul, Republic of Korea
[f] Cancer Research Institute, Seoul National University, Seoul, Republic of Korea
[g] Department of Physiology, School of Medicine, Pusan National University, Yangsan, Republic of Korea
[h] Genomic Medicine Institute, Medical Research Center, Seoul National University, Seoul, Republic of Korea
[i] Research Institute for Convergence of Biomedical Science and Technology, Pusan National University Yangsan Hospital, Yangsan, Republic of Korea

ARTICLE INFO

Keywords:
Alzheimer's disease
CD8$^+$ resident memory T cell
Choroid plexus epithelial cell
T cell exhaustion

ABSTRACT

Alzheimer's disease (AD) is a progressive neurological disorder and the leading cause of dementia. Despite significant efforts, treatment strategies targeting amyloid-β have been less successful than anticipated. Recently, the role of neuroinflammation and adaptive immune response in AD pathogenesis has gained attention. Here, we performed immune cell-enriched single-cell RNA sequencing of brain parenchymal cells from 12-month-old 5xFAD, an AD mouse model. We analyzed 11,587 single cells and found distinct differences in T cell and choroid plexus cell populations between 5xFAD mouse and littermate control. Subsequent sub-clustering of T cells in the 5xFAD mouse revealed distinct subtypes, with CD8$^+$ resident memory T cells (T_{RM}) being the most prevalent T cell type. In addition, we observed an increase in T cell exhaustion markers, including *Pdcd1, Ctla4, and Havcr2*, with a particularly significant elevation of PD-1 and TIM-3 in CD8$^+$ T_{RM} in 5xFAD mouse. Furthermore, choroid plexus (ChP) epithelial cells showed altered gene expression patterns, with higher expression of MHC class I and Type I IFN-stimulated genes in 5xFAD mouse compared to the control mouse, suggesting an association with clonal expansion of AD-specific T cells in the brain. Through single-cell RNA sequencing (scRNA-seq) analysis, our study highlights the potential role of resident memory CD8$^+$ T cell and their possible interactions with ChP epithelial cells. This study provides an exploration of the brain microenvironment landscape in AD, revealing critical insights into its underlying mechanisms.

1. Introduction

Neuroinflammation is one of the crucial pathogeneses in the progression of Alzheimer's disease (AD). Due to the long-held belief that the brain is immune-privileged, only the role of innate immunity (e.g. microglia) has been extensively investigated. However, it is now understood that the brain is under constant immune surveillance from both the innate and adaptive immune systems (Louveau et al., 2015). Despite the restricted access of adaptive immune cells through the blood-brain barrier, increasing evidence shows the presence of T cells in the brain

* Corresponding author at: Department of Biomedical Sciences, Seoul National University Graduate School, Seoul, Republic of Korea.
** Corresponding author at: Department of Physiology, School of Medicine, Pusan National University, Yangsan, Republic of Korea.
*** Corresponding author at: Department of Microbiology and Immunology, Seoul National University Graduate School, Seoul, Republic of Korea.
E-mail addresses: chgpark@snu.ac.kr (C.-G. Park), hyunsu.lee@pusan.ac.kr (H. Lee), tte9801@snu.ac.kr (H.J. Kim).
[1] Equal contribution.

https://doi.org/10.1016/j.jneuroim.2024.578488
Received 10 June 2024; Received in revised form 8 November 2024; Accepted 13 November 2024
Available online 17 November 2024

with their entry becoming more pronounced with aging (Togo et al., 2002; Stalder et al., 2005; Gemechu and Bentivoglio, 2012). These pieces of evidence suggest that T cells may play crucial modulating roles in both protection and neurological disease, including AD. For instance, infiltrating T cells were also associated with the disease progression (Togo et al., 2002; Stalder et al., 2005; Rogers et al., 1988; Browne et al., 2013; Ferretti et al., 2016; Unger et al., 2020). $CD8^+$ T cells have been observed in the hippocampus of both AD patients and tauopathy mouse models, correlating with disease severity and cognitive decline (Su et al., 2023; Chen et al., 2023). The infiltration of these T cells into the brain parenchyma suggests an interaction with resident immune cells, such as microglia and astrocytes, potentially exacerbating neuroinflammation and neuronal damage (Laurent et al., 2017). However, the phenotypic characteristics of infiltrating T cells and their interaction with non-immune cells in the brain which have a consequential impact on the progression of AD remain uncertain.

Amyloid-β accumulation, which is thought to drive the pathogenesis of AD, has been discovered in the choroid plexus (ChP) in addition to the brain parenchyma and blood vessels (Dietrich et al., 2008; Vargas et al., 2010). Moreover, morphological alterations have been detected in the choroid plexus in AD (Kant et al., 2018; Serot et al., 2000). The ChP serves as a blood-cerebrospinal fluid (CSF) barrier as well as a link for inflammatory signals between the brain and the periphery (Marques et al., 2009a; Marques et al., 2009b). These results suggest a potential role of the ChP in the brain's inflammatory response during the progression of AD. However, less attention has been given to how impaired ChP function contributes to the progression of neuroinflammation and the pathogenesis of AD.

To investigate the inflammatory micro milieu and further elucidate the role of immune cells in the interactions between the brain and immune cells, we performed immune cell-enriched single-cell RNA sequencing (scRNA-seq) using the 5xFAD mouse brain and age-matched control. We sought to gain a thorough understanding of the cellular landscape in the brain of the 5xFAD mouse, focusing especially on the immune cells that infiltrate the brain potentially contributing to the disease progression.

2. Materials and methods

2.1. Transgenic mice

5xFAD mice purchased from the Jackson Laboratory were utilized. These mice express mutant human amyloid precursor protein (APP) with three FAD mutations, the Swedish (K670N, M671L), Florida (I716V), and London mutation (V717I), as well as human presenilin 1 (PSEN1) with two FAD mutations (M146L and L286V). The mice were heterozygotes with respect to the transgene (Tg6799, B6/SJL hybrid background), and non-transgenic littermates were used as control. Animal care and use were in strict accordance with the Principal of Laboratory Animal Care (NIH publication) and the Animal Care and Use Guidelines of Seoul National University. All the experiments were approved by the Institutional Animal Care and Use Committee (IACUC) at Seoul National University, Seoul, Korea (IACUC Approval number: SNU-240328-2).

2.2. Brain-infiltrated immune cell enrichment using fluorescence-associated cell sorting

For scRNA-seq, brain-infiltrated cells were isolated from the 5xFAD mouse and its littermate. Mice were deeply anesthetized by IP injection of ketamine and xylazine. To remove the blood from circulation, mice were perfused with 1× HBSS for 5 min at a rate of 6 mL/min. Brain tissue was obtained from the mouse, chopped, and enzymatically digested with 0.1 % dispase and 0.3 % type 4 collagenase for 25 min. After mechanical digestion using a pipette-aid, the brain tissue was treated with DNase I for an additional 25 min. The dissociated brain was then centrifuged through 22.5 % Percoll gradient buffer for immune cell enrichment. Collected cells were stained with FVS700 (live/dead), anti-CD3 antibody, and anti-CD45 antibody. Among live cells, $CD45^{int/high}$ cells were sorted via BD FACSAria. Using sorted cells, Gell Bead-In Emulsion (GEM) processing, and cDNA library preparation was performed. Two brain samples were sequenced on an Illumina sequencing machine.

2.3. 10× genomics GEM generation, cDNA, library establishment

Single cell suspensions were loaded onto the 10× Chromium Controller according to the manufacturer's instructions for the Chromium Single Cell 5′ v2 kit. In brief, single cell suspensions and master mix were added to a Single Cell 5′ Chip along with the reverse transcription master mix and partitioning oil. The Chromium Controller generates GEMs, each containing a single cell and a barcoded bead for reverse transcription. Each bead carries oligos containing a 10× barcode, a unique molecular identifier (UMI), and poly-dT sequences to prime reverse transcription of poly-adenylated mRNA. After the GEM generation, GEMs were broken, and cDNA was cleaned up and amplified using a thermal cycler. Amplified cDNA products were sheared and size-selected to construct the sequencing library. The libraries were generated by attaching sequencing adapters and sample indices provided in the Chromium Single Cell 5′ v2 kit according to the manufacturer's instructions. Quality and quantity of the libraries were checked using the BioAnalyzer High Sensitivity DNA chip (Agilent).

2.4. 10× library sequencing

Prepared libraries were loaded onto an Illumina sequencing machine (NovaSeq 6000). Sequencing was performed according to the manufacturer's instructions to generate paired-end reads (Read1–28 bp; i7Index-8 bp; i5Index-0 bp; Read2-91 bp). Base calls by Illumina RTA were converted into FASTQ format via Illumina bcl2fastq software (version 2.20).

2.5. Quality control, cell grouping into subtypes, and analysis

To isolate healthy cells for analysis, specific criteria were implemented. Cells that expressed either more than 4000 or fewer than 800 unique genes were excluded to remove doublets and empty GEMs. To filter out apoptotic cells, any cells expressing mitochondrial genes of more than 5 % were also discarded.

Cells from the 12-month-old 5xFAD mouse model brain and cells from the control brain of same age were integrated as a whole, clustered into cell groups, and projected by uniform manifold approximation and projection (UMAP). For each cluster, differentially expressed genes were used as markers for cell-type annotation. T cell clusters were annotated using CD3, Ccl5, and Nkg7 (Zheng et al., 2017). Choroid plexus epithelial cell clusters were annotated using *Ttr*, *Mt3*, and *Ecrg4* (Gonzalez et al., 2011). To annotate other cell clusters, we referred to the following papers: (Ortiz-Alvarez et al., 2019; Redmond et al., 2019; Zareba and Kepinska, 2020; Vanlandewijck et al., 2018).

Analyses were performed to explore the potential communication between different cell types in 5xFAD mouse, a receptor-ligand interaction analysis was performed using R package CellChat (ver 1.5.0) package (Jin et al., 2021). For each signaling pathway, circular relationship graphs were generated, where cell types were represented as nodes connected by arrows. The direction of the arrows indicates the flow from ligand-expressing cells to receptor-expressing cells, with the thickness of the arrows representing the strength of the interaction.

2.6. Gene set enrichment analysis

Gene Set Enrichment Analysis (GSEA) was conducted using Metascape (https://metascape.org) on the differentially expressed genes

(DEGs) identified in 5xFAD and littermate control. The DEGs were categorized into up-regulated and down-regulated groups. For each group, enrichment analysis was performed using default settings in Metascape, which includes Gene Ontology (GO) terms, KEGG pathways, and other functional sets. The analysis was run against a background of all genes in the genome. Enriched terms were identified based on their statistical significance, represented as -log10(P) values. The top enriched terms for both up-regulated and down-regulated genes were visualized using bar charts, with the length of each bar corresponding to the -log10(P) value of the enrichment. This analysis revealed key biological processes and pathways that were significantly altered in the 5xFAD model, providing insights into the molecular mechanisms potentially involved in the disease progression.

2.7. Flow cytometry

Percoll-enriched cells isolated from the brains of 5xFAD mice and their littermates were used for flow cytometry staining. For each test, 10^6 cells were collected. Brain-infiltrating immune cells were isolated as described above. Staining was performed according to the manufacturer's protocols.

Zombie Aqua Fixable Viability Kit (Cat: 423101, Biolegend) was used to exclude dead cells. The following antibodies were used for cell surface staining: I-A/I-E (MHC II) BV786 (clone 2G9, BD OptiBuild, 743,875), CD3 BV605 (clone 145-2C11, BD Horizon, 563,004), CD11b PE-Cy5 (clone M1/70, eBioscience, 15–0112-82), CD25 Vio Bright R720 (clone REA568, Miltenyi, 130–127-476), CD103 BV711 (clone M290, BD Horizon, 564,320), CD8a PE-Cy5.5 (clone 53–6.7, eBioscience, 35–0081-82), CD279 (PD-1) PE (clone REA802, Miltenyi, 130–111-953), TIM3 (CD366) PE-Cy7 (clone RMT3–23, eBioscience, 25–5870-80), H-2Kb PerCP-Cy5.5 (clone AF6–88.5, Biolegend, 116,515), CD31 FITC (clone 390, Biolegend, 102,405), CD4 BV496 (clone GK1.5, BD, 612952), CD45 APC-Cy7 (clone 30-F11, Biolegend, 103,116), and CD69 Pacific Blue (clone H1.2F3, Biolegend, 104,524).

For intracellular staining of CTLA4, cells were fixed and permeabilized using the Foxp3/Transcription Factor Staining Buffer Set (eBioscience) according to the manufacturer's instructions. Cells were then stained with anti-CTLA4 (CD152) PE-CF594 (clone UC10-4F10–11, BD Horizon, 564,332).

2.8. Fluorescence microscopy

Fluorescence microscopy was performed on sagittal brain sections (6 μm) from 12-month-old male 5xFAD mice and littermate controls. Sections were stained with rabbit polyclonal anti-CD3 antibody (1:200, Dako, A0452) and rat monoclonal anti-CD8a antibody (clone 53–6.7, 1:200, Invitrogen, 16–0081-82). Secondary antibodies used were Goat anti-Rabbit IgG (H + L), Alexa Fluor 647 (1:500, Thermo Fisher Scientific, A-21244) and Goat anti-Rat IgG (H + L), Alexa Fluor 488 (1:500, Thermo Fisher Scientific, A-11006). respectively. DAPI was used for nuclear counterstaining. Images were acquired using an OLYMPUS IX-51 microscope with a 40× objective. Images were captured and analyzed using FluoView software.

2.9. Statistical analysis

Statistical analyses were performed with GraphPad Prism software (version 9, GraphPad, Inc., La Jolla, CA, USA). The comparisons between 5xFAD and their littermates were assessed using two-way unpaired *t*-test. Data were shown as the mean ± SEM.

3. Results

3.1. $CD45^+$ cell-enriched scRNA-seq analysis identified ten cellular subtypes residing in 5xFAD mouse brain

Given the complex nature of immune cell populations within the brain, it was crucial to segregate brain-infiltrating immune cells from the immune cells circulating in the blood to obtain a clear snapshot of the immune cell dynamics in the brain milieu. The analyses were successfully accomplished through a specialized procedure, which effectively differentiated these two cell populations (Fig. 1A). After the cell collection, a rigorous quality control assessment was carried out to ensure the reliability of the subsequent analyses. As a result, we analyzed a pool of 11,587 cells (5689 cells from the 5xFAD model and 5898 cells from the control) that passed this quality assessment, providing a broad spectrum for detailed investigation. Utilizing unsupervised clustering techniques, these cells were grouped into ten distinct sub-clusters (Fig. 1B). This initial segregation was instrumental in providing an overview of the various immune cell populations residing in the 5xFAD mouse brain. To further resolve the identities of these subclusters, an analysis of differentially expressed genes (DEGs) was performed (Fig. 1C). The comparison between 5xFAD and littermate control revealed distinct differences in the cell populations (Fig. 1D). Specifically, certain cell clusters, such as T cells, showed significant increases in the 5xFAD model. In contrast, other cell types, such as choroid plexus epithelial cells, seem to have a notable reduction in the 5xFAD (Fig. 1E). These alterations underscored the substantial reorganization of the brain's immune landscape in the context of the 5xFAD mouse, which may contribute to the pathogenesis and progression of Alzheimer's disease.

3.2. Altered ratio and increased expression of exhaustion markers in resident memory $CD8^+$ T cells of 5xFAD mouse brain

Since we observed significant shifts in the T cell population in the 5xFAD brain compared to the littermate control, we aimed to further analyze T cell subsets. As shown in the UMAP plot (Fig. 2A and D), T cells were significantly enriched in the 5xFAD mouse brain, constituting 29.62 % of the total immune-enriched cells (1685 cells) compared to only 2.75 % in the littermate control (162 cells). Fluorescence microscopy analysis further confirmed this T cell enrichment. Sagittal sections of mouse brain parenchymal tissue between the hippocampus and ventricle were examined at 400× magnification using CD3 (red) and CD8 (green) markers, with DAPI for nuclear staining. The 5xFAD mouse brain exhibited a marked increase in $CD3^+$ T cells compared to the littermate control, with a notable subset of $CD8^+$ T cells. These images revealed clusters of T cells scattered throughout the parenchyma, particularly in the 5xFAD mouse brain, whereas, the littermate control showed less T cell presence (Supplementary Fig. 1 A). This contrast highlights the significant redistribution of immune cell populations in the context of Alzheimer's disease, suggesting that the immune environment in the 5xFAD mouse brain is markedly different from that of the littermate control (Fig. 1D, E). Further analysis of the T cell populations revealed distinct subtypes within this group. The T cells were separated into a new Seurat object, and re-clustered, resulting in the identification of seven discrete T cell subtypes. T cells were subclustered using specific markers to identify distinct populations (Fig. 2B). $CD8^+$ resident memory T cells (T_{RM}) were defined as $CD8^+CD69^+CD103^+$, with a subset further characterized as IFN-stimulated gene-high $CD8^+$ T_{RM} (CD8 IFN+ T_{RM}). Interestingly, a predominance of $CD8^+$ cells over $CD4^+$ cells was observed, a profile not typically seen in peripheral blood or spleen (Amadori et al., 1995). Flow cytometry validation at the protein level confirmed a higher proportion of $CD8^+CD69^+CD103^+$ T_{RM} cells in 5xFAD brains compared to littermate controls (Fig. 2C, $p = 0.1247$). UMAP visualization of T cell distributions in 5xFAD and littermate brains (Fig. 2D) further emphasized the expansion of $CD8^+$ TRM and

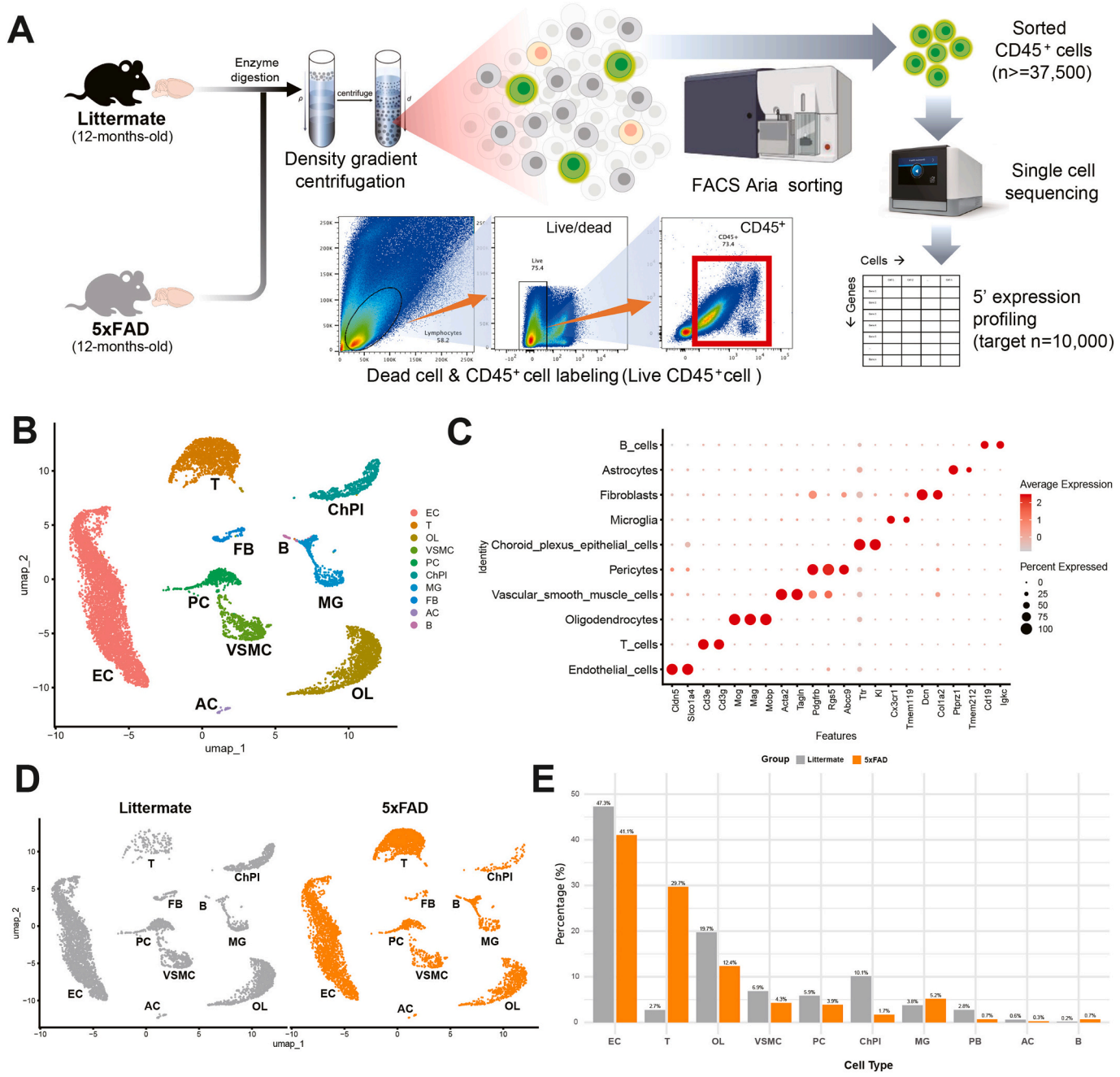

Fig. 1. Single cell transcriptomics identified brain cellular alterations in the 5xFAD mouse compared to its littermate (A) Schematic overview of the experimental procedure. Whole brains from 12-month-old 5xFAD and littermate control animals were harvested and processed. The brains were digested into single-cell suspensions, and live CD45^{+} immune cells were isolated using density gradient centrifugation followed by Fluorescence-Activated Cell Sorting (FACS). The sorted cells were subjected to single-cell RNA sequencing (scRNA-seq) using the 10× Genomics 5' RNA sequencing platform. This approach allowed for the capture of the transcriptomes of individual immune cells. (B) Uniform Manifold Approximation and Projection (UMAP) clustering of immune cells. UMAP analysis was used to visualize and cluster the immune cells from the scRNA-seq data. Ten distinct immune cell subtypes were identified based on their transcriptomic profiles. Each cluster represents a specific immune cell population present in the brain samples from the 5xFAD and littermate control. (C) A DotPlot showing the expression levels of key differentially expressed genes (DEGs) across the identified immune cell subtypes. The size of each dot indicates the proportion of cells within each subtype expressing the gene, while the color intensity represents the average expression level. This analysis was used to annotate the cellular subtypes based on their gene expression signatures. (D) UMAP clustering results separated by the 5xFAD and littermate control conditions. This panel shows the distribution and abundance of immune cell populations in each condition, enabling a comparison of immune cell profiles between the two groups. (E) A bar graph representing the relative percentage of each immune cell subpopulation identified in the 5xFAD and littermate control samples. This graph provides a quantitative view of the differences in the proportions of immune cell types between the two groups.

CD8^{+} IFN+ T_{RM} populations in the 5xFAD model. Differential gene expression analysis between 5xFAD and littermate CD8^{+} T cells revealed significant alterations in immune-related pathways. Volcano plot and GO pathway analysis (Fig. 2E) showed upregulation of genes associated with adaptive immune response and lymphocyte activation in 5xFAD brain. Notably, exhaustion markers (*Pdcd1, Havcr2, Ctla4*) and other T cell functional genes (*Itgae, Gzmb, Prf1*) were significantly upregulated in 5xFAD CD8^{+} T cells (Fig. 2F). Flow cytometry further validated the

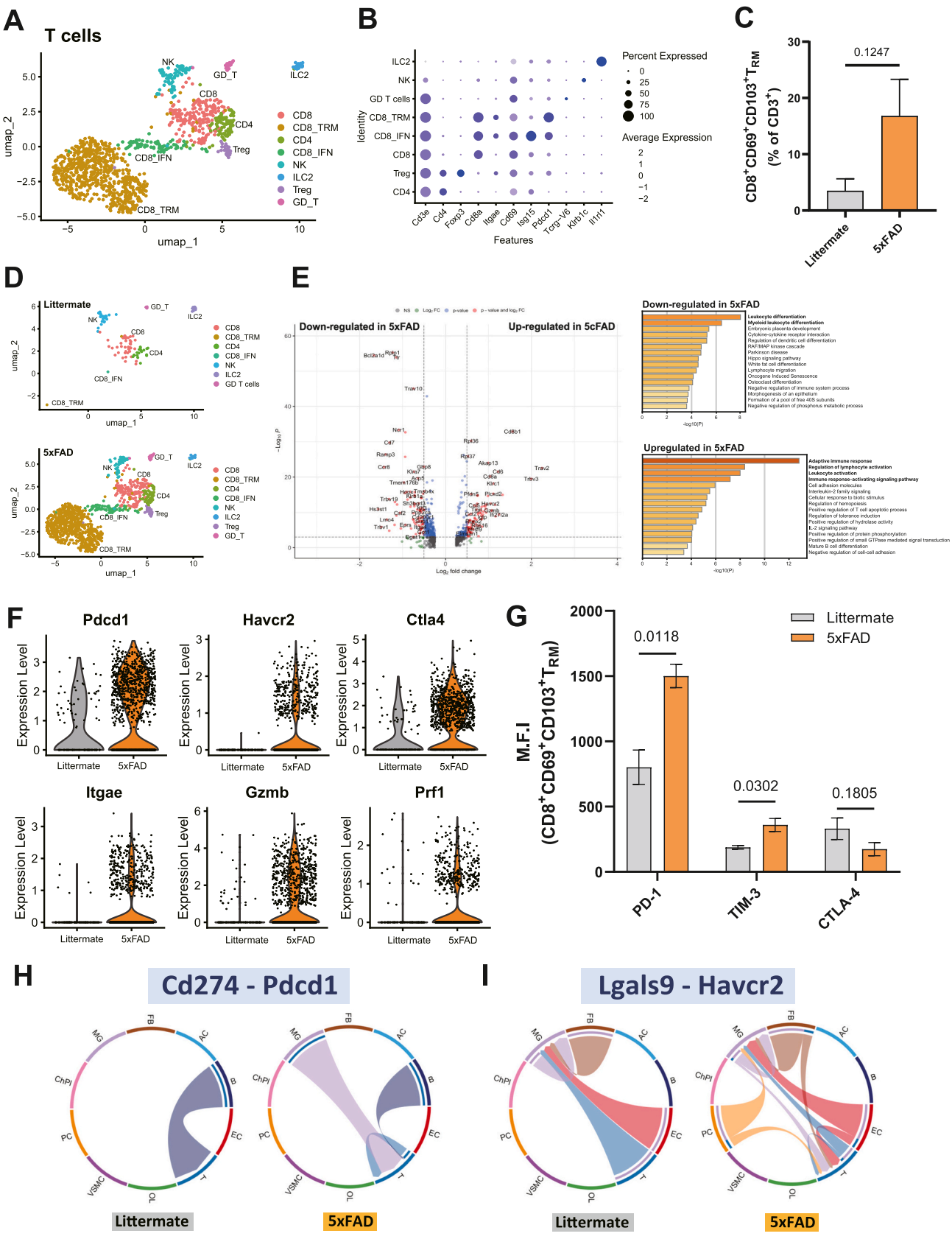

(caption on next page)

Fig. 2. Resident memory CD8$^+$ T cells exhibited altered ratio and increased expression of exhaustion markers in 5xFAD mouse (A) UMAP visualization of T cell populations identified by single-cell RNA sequencing. T cells were clustered based on their transcriptomic profiles, revealing distinct subpopulations of T cells within the sample. (B) Dot plot of gene expression across T cell subsets. The dot plot illustrates the expression levels of key genes in the identified T cell subpopulations. The size of the dots corresponds to the percentage of cells expressing the gene, and the color intensity reflects the average expression level within the subpopulation. (C) Quantification of CD8$^+$CD69$^+$CD103$^+$ tissue-resident memory (TRM) T cells as a percentage of total CD3$^+$ T cells in littermate and 5xFAD samples. Data are shown for three biological replicates per group ($n = 3$). Statistical significance was determined using an unpaired *t*-test. (D) UMAP plots of T cell populations split by condition. Top: T cell population distribution in littermate controls. Bottom: T cell population distribution in 5xFAD. The UMAP visualizes changes in T cell subpopulations between the two conditions. (E) Differential gene expression analysis between 5xFAD and littermate conditions. Left: Volcano plot showing differentially expressed genes, with the x-axis representing the log2 fold change and the y-axis showing the -log10(*p*-value). Right: Gene Set Enrichment Analysis (GSEA) results, with the top enriched pathways shown for both down-regulated (top) and up-regulated (bottom) genes in 5xFAD. (F) Violin plots of gene expression levels for key immune-related genes. Expression levels of *Pdcd1*, *Havcr2*, *Ctla4*, *Itgae*, *Gzmb*, and *Prf1* are shown in littermate and 5xFAD samples. Statistical significance was determined using the Wilcoxon rank-sum test. (G) Mean fluorescence intensity (MFI) of PD-1, TIM-3, and CTLA-4 in CD8$^+$CD69$^+$CD103$^+$ T cells from littermate and 5xFAD samples. Data are represented as the MFI, with statistical significance determined using an unpaired *t*-test ($n = 3$ per group). (H-I) CellChat analysis of ligand-receptor interactions. Circular plots show cell-cell communication patterns for the Cd274-Pdcd1 (H) and Lgals9-Havcr2 (I) ligand-receptor pairs in littermate and 5xFAD conditions. Circles represent the different cell types: ChP (choroid plexus), EC (endothelial cells), OL (oligodendrocytes), PC (pericytes), VSMC (vascular smooth muscle cells), FB (fibroblasts), MG (microglia), T (T cells), B (B cells), PC (Pericytes) and AC (astrocytes). These plots visualize the interactions between cells in the context of the respective ligand-receptor signaling pathways.

increased expression of PD-1 and TIM-3 at the protein level of 5xFAD CD8$^+$ T_{RM} cells (Fig. 2G, PD-1: $p = 0.0118$, TIM-3: $p = 0.0302$). Cell-to-cell interaction analysis using CellChat illustrated an obvious increase of communication, especially among T cells and other cell populations in the brain of 5xFAD mouse (Supplementary Fig. 2 A). Furthermore, in parallel with the exhaustion markers expression, enhanced interactions in T cells with other cell types via PD-1 (*Cd274-Pdcd1*) and TIM-3 (*Lgals9-Havcr2*) from 5xFAD brain compared to littermate control was also observed (Fig. 2H-I). Together, these results suggest the enrichment of CD8$^+$ T_{RM} cells in 5xFAD brains, along with enhanced cell-cell interactions, might potentially alter cell function, such as exhaustion markers elevation.

3.3. MHC class I and type 1 IFN response genes were highly expressed in choroid plexus epithelial cells of 5xFAD mouse

The choroid plexus is an epithelial tissue that lines the ventricles of the brain and is responsible for the production of CSF. Alongside its barrier function, the ChP epithelium acts as an interface between the brain and the immune system, facilitating immune cell trafficking and immune mediator secretion (Meeker et al., 2012). Indeed, we observed a diminished population of ChP epithelial cells (Fig. 1D). Therefore, we conducted further analysis of this sub-cluster. When we depicted the UMAP of ChP epithelial cells exclusively, the significant decrease of this subcluster could be visualized more distinctly (Fig. 3A-B). The violin plot (Fig. 3C) revealed that MHC class I genes, such as *B2m* and *Tapbp*, as well as type 1 IFN response genes, such as *Irf7* and *Isg15*, were upregulated in ChP epithelial cells of 5xFAD mouse compared to its littermate control. Next, the expression of MHC class I at the protein level of the CD31$^-$CD45$^-$CD11b$^-$ subset, which contains the ChP epithelial cells, was examined by flow cytometry. MHC-I was significantly increased in 5xFAD (Fig. 3D). In agreement with protein expression level, the cell-to-cell interaction analysis indicated an overall significant upregulation of the MHC class I signaling pathway in the 5xFAD mouse (Fig. 3E). Moreover, the VCAM-1 signaling pathway was notably enhanced among interactions between ChP and T cells, Microglia cells, and vascular smooth muscle cells (Fig. 3F). Collectively, these data revealed an alteration in the ChP epithelial cells frequency, and their increased expression of MHC class I and VCAM pathways in the brain of 5xFAD mouse, which may be related to AD pathogenesis and is highly likely to influence the CD8$^+$ T_{RM} cells.

4. Discussion

There is considerable evidence that T cells infiltrate the brains of AD patients (Togo et al., 2002; Rogers et al., 1988) and AD mouse models (Stalder et al., 2005; Browne et al., 2013; Ferretti et al., 2016; Unger et al., 2020). In a human study, an increase in the number of CD8$^+$ T effector memory cells (CD45RA$^+$) was associated with cognitive decline in an AD cohort (Gate et al., 2020). In vivo studies showed that T cell infiltration exacerbated spatial memory impairment by enhancing the innate neuroinflammatory response in a tau transgenic mouse (Laurent et al., 2017). In the APP/PS1 mouse model, the introduction of amyloid-β-immunized CD4$^+$ T cells or CD4$^+$ effector T cells was reported to impair cognitive function (Browne et al., 2013; Machhi et al., 2021). Depletion of CD4$^+$ T regulatory cells accelerated cognitive function decline, whereas, an increased number of T regulatory cells with low-dose IL-2 treatment improved cognitive function (Dansokho et al., 2016). These consistent findings suggest that the role of T cell infiltration in AD progression may depend on the specific T cell subtype and the stage of the disease. Among the CD8$^+$ T memory cells, the key subtypes are effector memory T cells, central memory T cells, and T_{RM} cells (Martin and Badovinac, 2018). T_{RM} cells, characterized by the expression of integrins, such as CD103 and CD49a, are primarily found in chronic inflammatory peripheral organs (Samat et al., 2021). Prior studies demonstrated an elevation of CD8$^+$ T_{RM} cells that expressed CXCR6, CD103, CD69, and PD-1 in different AD mouse models (Altendorfer et al., 2022). Consistently, we also found an increased number of T cells in the brain of a 12-month-old 5xFAD mouse compared to its littermate, with the majority of CD8$^+$ T cell subsets. Though CD8$^+$ T cells are supposed to elevate in general with aging (Su et al., 2023), those in 5xFAD are far more numerous than those of the age-matched and sex-matched littermate. Thus, it is highly likely that they are involved in the disease pathogenesis rather than aging. Since a 5xFAD mouse was used, the imbalances in CD8$^+$ T cells might be limited to amyloid plaque pathology. Given a clearer association of CD8$^+$ T in tau pathology, further studies may discover more pronounced CD8+ T imbalances using a model that includes tau pathology.

Despite the importance of studying T cell exhaustion, a keyword in immune dysfunction in chronic inflammatory diseases and tumors, research on this topic is particularly limited in AD (McKinney and Smith, 2016; Gao et al., 2022; Zarour, 2016; Tabana et al., 2021). A previous study found an increased proportion of exhausted T cells in the peripheral blood from patients with AD (Wu et al., 2021). In AD mouse models, an increase of PD-1$^+$ co-expressing CXCR6 on CD8$^+$ T cells was reported in 5xFAD mice, indicating a protective function (Su et al., 2023). However, the similar population in ET5 mice was suggested to promote disease (Chen X et al., 2023). Although their studies were conducted in different transgenic mouse models, the controversial observation might suggest the microenvironment-dependent functions of the same cell subset. Our data also observed a similarly increased expression of PD-1 in CD8$^+$ T_{RM}, which co-expressed CD69 and CD103 in the brains of 8-month-old 5xFAD mice. Expanding on previous reports, we detected an increased proportion of exhaustion marker-expressing CD8$^+$ T_{RM} cells within the brain of 5xFAD mouse, including *Pdcd1*, *Ctla4*, and *Havcr2* at the mRNA level and PD-1 and

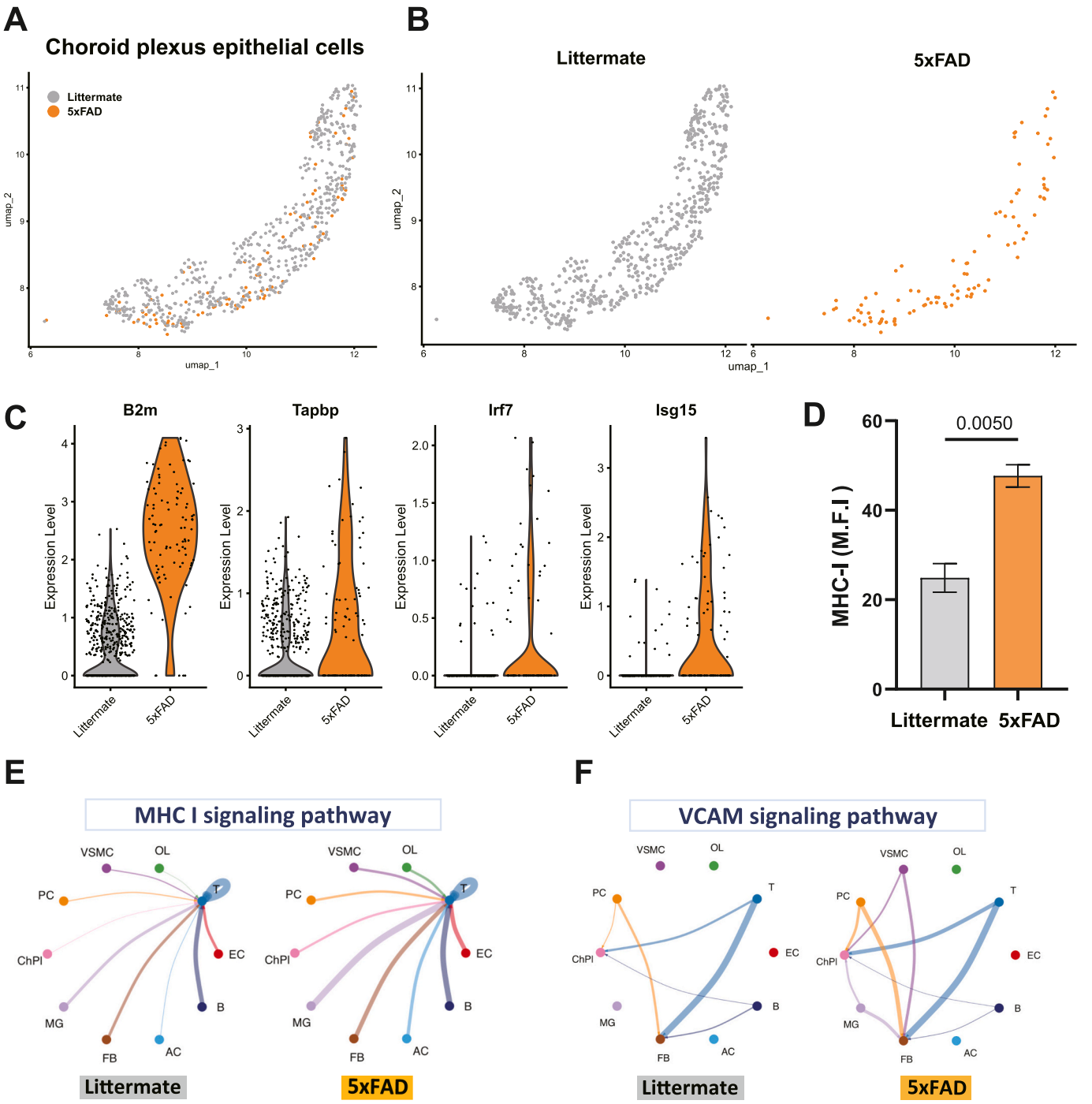

Fig. 3. Choroid plexus epithelial cells showed decreased ratio but elevated expression of MHC class I in 5xFAD mouse (A) UMAP visualization of choroid plexus epithelial cells from littermate (gray) and 5xFAD (orange) samples. The UMAP plot shows the clustering and distribution of choroid plexus epithelial cells from both conditions based on their transcriptomic profiles. (B) Separate UMAP plots for choroid plexus epithelial cells in littermate (left) and 5xFAD (right) conditions. These plots display the cell distribution within each group individually to highlight differences in clustering patterns between the two conditions. (C) Violin plots of gene expression levels for B2m, Tapbp, Irf7, and Isg15 in choroid plexus epithelial cells from littermate and 5xFAD samples. The violin plots show the distribution of gene expression levels, with each dot representing a single cell. Statistical significance was determined using the Wilcoxon rank-sum test. (D) Quantification of MHC-I mean fluorescence intensity (MFI) in choroid plexus epithelial cells from littermate and 5xFAD samples. Data are presented as mean ± SEM for $n = 3$ biological replicates per group. The p-value was determined using an unpaired t-test to compare MFI levels between the two groups. CellChat analysis of (E) MHC I and (F) VCAM signaling pathway interactions between different cell types in littermate (left) and 5xFAD (right) conditions. Circles represent the different cell types: ChP (choroid plexus), EC (endothelial cells), OL (oligodendrocytes), PC (pericytes), VSMC (vascular smooth muscle cells), FB (fibroblasts), MG (microglia), T (T cells), B (B cells), PC (Pericytes) and AC (astrocytes). Line thickness indicates the strength of the ligand-receptor interaction between cell types.

TIM-3 at the protein level compared to their littermates. Interestingly, in addition to the interaction between the T cell and Microglia clusters, which was previously reported (Altendorfer et al., 2022), receptor-ligand interaction analysis illustrated the interaction between the T cell cluster and other non-immune cell clusters in 5xFAD mice, but not in its littermate. This includes inflamed endothelial cells (via *Cd274* – *Pdcd1* and *Lgals9* – *Havcr2* signaling), stressed endothelial cells, and fibroblasts (via *Lgals9* – *Havcr2*). Thus, further investigation into the link between T cells, possibly the $CD8^+$ T_{RM} subset, and pathogenic endothelial cells or fibroblasts might expand our knowledge of the Aβ-associated AD pathogenesis.

The ChP epithelial cell layer plays a critical role in maintaining brain homeostasis, including immune cell infiltration restriction, toxic substances removal, and metabolite exchange (Ghersi-Egea et al., 2018). By using immune-enriched brain parenchymal cells without getting rid of the meninges, our study revealed a decrease in ChP epithelial cell numbers and an increase in MHC gene expression in the brain of late-phase 5xFAD mouse compared to its littermate control. Though our study has the limitation of not physically separating the meninges, these findings align with previous reports of morphological changes and inflammation in the ChP of patients with AD (Serot et al., 2000; Serot et al., 1994; Carna et al., 2023). For instance, studies have reported accelerated ChP epithelial cell atrophy in patients with AD, possibly due to A-beta toxicity, increased reactive oxygen species, and caspase-dependent apoptosis resulting from mitochondrial dysfunction (Vargas et al., 2010; Serot et al., 2000). Inflammatory changes in the CSF are also believed to contribute to ChP epithelial pathology (Carna et al., 2023). Previous research has observed MHC II^+ macrophages in the ChP stroma and MHC II expression in ChP epithelial cells in post-mortem tissue from patients with AD (Serot et al., 1994). The changes observed in the choroid plexus epithelial cells may reflect alterations in blood-CSF barrier integrity and immune cell recruitment (Schwartz and Baruch, 2014). In this study, we demonstrated a significant increase of MHC-I protein expression in the $CD31^-CD45^-CD11b^-$ population, which includes a proportion of ChP epithelial cells, in the brains of 8-month-old 5xFAD mice along with increased MHC gene expression in the brain of 12-month-old 5xFAD mouse. These findings suggest that the expression of MHC class I genes and type 1 IFN response genes by ChP epithelial cells may contribute to the neuroinflammatory response in AD. Indeed, prolonged exposure to antigens presented by MHC class I in the tumor microenvironment results in impaired effector functions of $CD8^+$ T cells, a state known as exhaustion, characterized by high expression levels of inhibitory receptors, such as PD-1, LAG-3, and TIM-3 (Baessler and Vignali, 2024). In the context of AD, $CD8^+$ T cells have been reported to interact primarily with microglia and play a significant role in the disease's pathology (Hu and Weiner, 2024). Here, our data suggest that the reduction of ChP epithelial cells, along with the upregulation of MHC class I and VCAM signaling pathways, may also be associated with $CD8^+$ T cell infiltration and function within the brain of the 5xFAD mouse. Although ChP do not directly interact with $CD8^+$ T cells through the exhaustion pathway, instead, increased infiltration of $CD8^+$ T cells and enhanced interaction with ChP epithelial cells via prolonged antigens exposure may contribute to AD pathogenesis and the eventual elevation of exhaustion markers in $CD8^+$ T_{RM} (Richter et al., 2012). Indeed, the VCAM signaling pathway, which might support the prolonged engagement with T cell receptor, was enhanced in 5xFAD mouse, particularly in interactions between T cells and ChP, while it remained unchanged between T cells and FB compared to the littermate control. In addition, those interactions between the two cell types might have led to some detrimental effects on ChP epithelial cells, resulting in a decrease in their numbers over time. In this study, beside the ChP – T cells communication, we also observed the interactions among T cells and other cell populations highlighting the importance of the tissue niche in shaping immune responses and contributing to AD pathogenesis (Hu and Weiner, 2024). Further studies utilizing spatial-based technologies are required to clarify the role of interactions between ChP epithelial cells and $CD8^+$ T_{RM}, particularly $CD69^+CD103^+$ $CD8^+$ T_{RM} in neuroinflammation and neuronal damage.

In conclusion, by utilizing scRNA-seq analysis on immune cell-enriched brain parenchyma in the 5xFAD mouse model, we explored an exhausted subset of $CD8^+$ T_{RM} cells and their potential connection with other non-immune cells, including inflamed endothelial cells, stressed endothelial cells, fibroblasts, and ChP epithelial cells. These findings may provide insight into the pathogenesis of AD.

Data sharing statement

The authors declare that all the data supporting the findings in this study are available from the corresponding author upon reasonable request.

Funding

This work was supported by the PB Immune Therapeutics, Seoul, Republic of Korea [grant number PB-2022-0004].

CRediT authorship contribution statement

Seong-Jun Kang: Writing – review & editing, Writing – original draft, Visualization, Methodology, Conceptualization. **Yong-Hee Kim:** Writing – review & editing. **Thuy Nguyen-Phuong:** Writing – review & editing, Data curation. **Yijoon Kim:** Formal analysis, Data curation. **Jin-Mi Oh:** Resources. **Jae-chun Go:** Writing – review & editing. **DaeSik Kim:** Writing – review & editing, Data curation. **Chung-Gyu Park:** Writing – review & editing, Supervision, Funding acquisition, Conceptualization. **Hyunsu Lee:** Writing – review & editing, Writing – original draft, Visualization, Supervision. **Hyun Je Kim:** Writing – review & editing, Supervision, Resources, Funding acquisition.

Declaration of competing interest

The authors declare that they have no conflict of interest.

Data availability

Data will be made available on request.

Acknowledgement

This research was supported by the PB Immune Therapeutics Academic Research Fund (PB-2022-0004).

Appendix A. Supplementary data

Supplementary data to this article can be found online at https://doi.org/10.1016/j.jneuroim.2024.578488.

References

Altendorfer, B., et al., 2022. Transcriptomic profiling identifies CD8(+) T cells in the brain of aged and Alzheimer's disease transgenic mice as tissue-resident memory T cells. J. Immunol. 209 (7), 1272–1285.
Amadori, A., et al., 1995. Genetic control of the CD4/CD8 T-cell ratio in humans. Nat. Med. 1 (12), 1279–1283.
Baessler, A., Vignali, D.A.A., 2024. T cell exhaustion. Annu. Rev. Immunol. 42 (1), 179–206.
Browne, T.C., et al., 2013. IFN-gamma production by amyloid beta-specific Th1 cells promotes microglial activation and increases plaque burden in a mouse model of Alzheimer's disease. J. Immunol. 190 (5), 2241–2251.
Carna, M., et al., 2023. Pathogenesis of Alzheimer's disease: involvement of the choroid plexus. Alzheimers Dement. 19 (8), 3537–3554.
Dansokho, C., et al., 2016. Regulatory T cells delay disease progression in Alzheimer-like pathology. Brain 139 (Pt 4), 1237–1251.
Dietrich, M.O., et al., 2008. Megalin mediates the transport of leptin across the blood-CSF barrier. Neurobiol. Aging 29 (6), 902–912.

Ferretti, M.T., et al., 2016. T-cell brain infiltration and immature antigen-presenting cells in transgenic models of Alzheimer's disease-like cerebral amyloidosis. Brain Behav. Immun. 54, 211–225.
Gao, Z., et al., 2022. T-cell exhaustion in immune-mediated inflammatory diseases: new implications for immunotherapy. Front. Immunol. 13, 977394.
Gate, D., et al., 2020. Clonally expanded CD8 T cells patrol the cerebrospinal fluid in Alzheimer's disease. Nature 577 (7790), 399–404.
Gemechu, J.M., Bentivoglio, M., 2012. T cell recruitment in the brain during Normal aging. Front. Cell. Neurosci. 6, 38.
Ghersi-Egea, J.F., et al., 2018. Molecular anatomy and functions of the choroidal blood-cerebrospinal fluid barrier in health and disease. Acta Neuropathol. 135 (3), 337–361.
Gonzalez, A.M., et al., 2011. Ecrg4 expression and its product augurin in the choroid plexus: impact on fetal brain development, cerebrospinal fluid homeostasis and neuroprogenitor cell response to CNS injury. Fluids Barriers CNS 8 (1), 6.
Hu, D., Weiner, H.L., 2024. Unraveling the dual nature of brain CD8(+) T cells in Alzheimer's disease. Mol. Neurodegener. 19 (1), 16.
Jin, S., et al., 2021. Inference and analysis of cell-cell communication using CellChat. Nat. Commun. 12 (1), 1088.
Kant, S., et al., 2018. Choroid plexus genes for CSF production and brain homeostasis are altered in Alzheimer's disease. Fluids Barriers CNS 15 (1), 34.
Laurent, C., et al., 2017. Hippocampal T cell infiltration promotes neuroinflammation and cognitive decline in a mouse model of tauopathy. Brain 140 (1), 184–200.
Louveau, A., et al., 2015. Structural and functional features of central nervous system lymphatic vessels. Nature 523 (7560), 337–341.
Machhi, J., et al., 2021. CD4+ effector T cells accelerate Alzheimer's disease in mice. J. Neuroinflammation 18 (1), 272.
Marques, F., et al., 2009a. The choroid plexus response to a repeated peripheral inflammatory stimulus. BMC Neurosci. 10, 135.
Marques, F., et al., 2009b. Kinetic profile of the transcriptome changes induced in the choroid plexus by peripheral inflammation. J. Cereb. Blood Flow Metab. 29 (5), 921–932.
Martin, M.D., Badovinac, V.P., 2018. Defining memory CD8 T cell. Front. Immunol. 9, 2692.
McKinney, E.F., Smith, K.G., 2016. T cell exhaustion and immune-mediated disease-the potential for therapeutic exhaustion. Curr. Opin. Immunol. 43, 74–80.
Meeker, R.B., et al., 2012. Cell trafficking through the choroid plexus. Cell Adh. Migr. 6 (5), 390–396.
Ortiz-Alvarez, G., et al., 2019. Adult neural stem cells and multiciliated ependymal cells share a common lineage regulated by the geminin family members. Neuron 102 (1), 159–172 e7.
Redmond, S.A., et al., 2019. Development of ependymal and postnatal neural stem cells and their origin from a common embryonic progenitor. Cell Rep. 27 (2), 429–441 e3.
Richter, K., Brocker, T., Oxenius, A., 2012. Antigen amount dictates CD8+ T-cell exhaustion during chronic viral infection irrespective of the type of antigen presenting cell. Eur. J. Immunol. 42 (9), 2290–2304.
Rogers, J., et al., 1988. Expression of immune system-associated antigens by cells of the human central nervous system: relationship to the pathology of Alzheimer's disease. Neurobiol. Aging 9 (4), 339–349.
Samat, A.A.K., et al., 2021. Tissue-resident memory T cells in chronic inflammation-local cells with systemic effects? Cells 10 (2).
Schwartz, M., Baruch, K., 2014. The resolution of neuroinflammation in neurodegeneration: leukocyte recruitment via the choroid plexus. EMBO J. 33 (1), 7–22.
Serot, J.M., Bene, M.C., Faure, G.C., 1994. Comparative immunohistochemical characteristics of human choroid plexus in vascular and Alzheimer's dementia. Hum. Pathol. 25 (11), 1185–1190.
Serot, J.M., et al., 2000. Morphological alterations of the choroid plexus in late-onset Alzheimer's disease. Acta Neuropathol. 99 (2), 105–108.
Stalder, A.K., et al., 2005. Invasion of hematopoietic cells into the brain of amyloid precursor protein transgenic mice. J. Neurosci. 25 (48), 11125–11132.
Tabana, Y., et al., 2021. Reversing T-cell exhaustion in immunotherapy: a review on current approaches and limitations. Expert Opin. Ther. Targets 25 (5), 347–363.
Togo, T., et al., 2002. Occurrence of T cells in the brain of Alzheimer's disease and other neurological diseases. J. Neuroimmunol. 124 (1–2), 83–92.
Unger, M.S., et al., 2020. CD8(+) T-cells infiltrate Alzheimer's disease brains and regulate neuronal- and synapse-related gene expression in APP-PS1 transgenic mice. Brain Behav. Immun. 89, 67–86.
Vanlandewijck, M., et al., 2018. A molecular atlas of cell types and zonation in the brain vasculature. Nature 554 (7693), 475–480.
Vargas, T., et al., 2010. Abeta accumulation in choroid plexus is associated with mitochondrial-induced apoptosis. Neurobiol. Aging 31 (9), 1569–1581.
Wu, Q., Kong, W., Wang, S., 2021. Peripheral blood biomarkers CXCL12 and TNFRSF13C associate with cerebrospinal fluid biomarkers and infiltrating immune cells in Alzheimer disease. J. Mol. Neurosci. 71 (7), 1485–1494.
Zareba, N., Kepinska, M., 2020. The function of transthyretin complexes with Metallothionein in Alzheimer's disease. Int. J. Mol. Sci. 21 (23).
Zarour, H.M., 2016. Reversing T-cell dysfunction and exhaustion in Cancer. Clin. Cancer Res. 22 (8), 1856–1864.
Zheng, C., et al., 2017. Landscape of infiltrating T cells in liver Cancer revealed by single-cell sequencing. Cell 169 (7), 1342–1356 e16.